Medical Image Analysis 63 (2020) 101709

Contents lists available at ScienceDirect

Medical Image Analysis

journal homepage: www.elsevier.com/locate/media

Designing weighted correlation kernels in convolutional neural networks for functional connectivity based brain disease diagnosis

Biao Jie[a,b,1], Mingxia Liu[b,1], Chunfeng Lian[b], Feng Shi[c], Dinggang Shen[b,d,*]

[a] School of Computer and Information, Anhui Normal University, Anhui 241003, China
[b] Department of Radiology and BRIC, University of North Carolina at Chapel Hill, North Carolina 27599, USA
[c] Shanghai United Imaging Intelligence Co., Ltd., Shanghai 201807, China
[d] Department of Brain and Cognitive Engineering, Korea University, Seoul, Korea

ARTICLE INFO

Article history:
Received 27 February 2019
Revised 10 October 2019
Accepted 15 April 2020
Available online 23 April 2020

Keywords:
Functional connectivity network
Correlation kernel
Convolutional neural network
Alzheimer's disease
Classification

ABSTRACT

Functional connectivity networks (FCNs) based on functional magnetic resonance imaging (fMRI) have been widely applied to analyzing and diagnosing brain diseases, such as Alzheimer's disease (AD) and its prodrome stage, *i.e.*, mild cognitive impairment (MCI). Existing studies usually use Pearson correlation coefficient (PCC) method to construct FCNs, and then extract network measures (*e.g.*, clustering coefficients) as features to learn a diagnostic model. However, the valuable observation information in network construction (*e.g.*, specific contributions of different time points), as well as high-level and high-order network features are neglected in these studies. In this paper, we first define a novel weighted correlation kernel (called wc-kernel) to measure the correlation of brain regions, by which weighting factors are learned in a data-driven manner to characterize the contributions of different time points, thus conveying the richer interaction information among brain regions compared with the PCC method. Furthermore, we build a wc-kernel based convolutional neural network (CNN) (called wck-CNN) framework for learning the hierarchical (*i.e.*, from local to global and also from low-level to high-level) features for disease diagnosis, by using fMRI data. Specifically, we first define a layer to build dynamic FCNs using our proposed wc-kernels. Then, we define another three layers to sequentially extract local (brain region specific), global (brain network specific) and temporal features from the constructed dynamic FCNs for classification. Experimental results on 174 subjects (a total of 563 scans) with rest-state fMRI (rs-fMRI) data from ADNI database demonstrate the efficacy of our proposed method.

1. Introduction

Accurate diagnosis of brain diseases, such as Alzheimer's disease (AD) and its prodromal stage, *i.e.*, mild cognitive impairment (MCI), is very important for early treatment and possible delay of disease progression. As a complex network, the human brain contains a large number of functional regions. The functional interaction among these regions provides an important insight into the basic mechanism and cognitive processes of the brain (Greicius et al., 2003). In the context of neuroimaging, functional magnetic resonance imaging (fMRI) provides a non-invasive way to map the functional interaction of the brain. Based on fMRI data, functional connectivity networks (FCNs), which characterize functional interactions among brain regions, have been applied to brain disease analysis, and thus helping us better understand the pathology of neurological disorders. Recently, FCNs constructed based on resting-state fMRI (rs-fMRI) have been widely applied in the task of automated brain diseases diagnosis (Guye et al., 2010; Jie et al., 2014a; Wee et al., 2012a).

Up to now, studies on FCNs typically focus on two aspects: 1) *traditional FCN*, which usually implicitly assumes that functional connectivity is temporally stationary throughout recording period in fMRI (Sporns, 2011). However, these studies ignore the changing properties of FCNs over time. 2) *dynamic FCN*, which focuses on the temporal changes of functional connectivity between specific brain regions. Existing studies have suggested that the changing properties of functional connectivity over time may be associated with cognitive and vigilance state (Thompson et al., 2013; Chang et al., 2013), which are critical for better understanding the pathology of brain diseases (Hutchison et al., 2013; Zhang and Small, 2006; Kiviniemi et al., 2011). Also, some studies have found that brain diseases (*e.g.*, AD/MCI) are related with temporal changes of functional connectivities (Jones et al., 2012; Wee et al., 2016).

* Corresponding author.
E-mail addresses: jbiao@nuaa.edu.cn (B. Jie), dgshen@med.unc.edu (D. Shen).
[1] These authors contributed equally to this paper.

https://doi.org/10.1016/j.media.2020.101709
1361-8415/

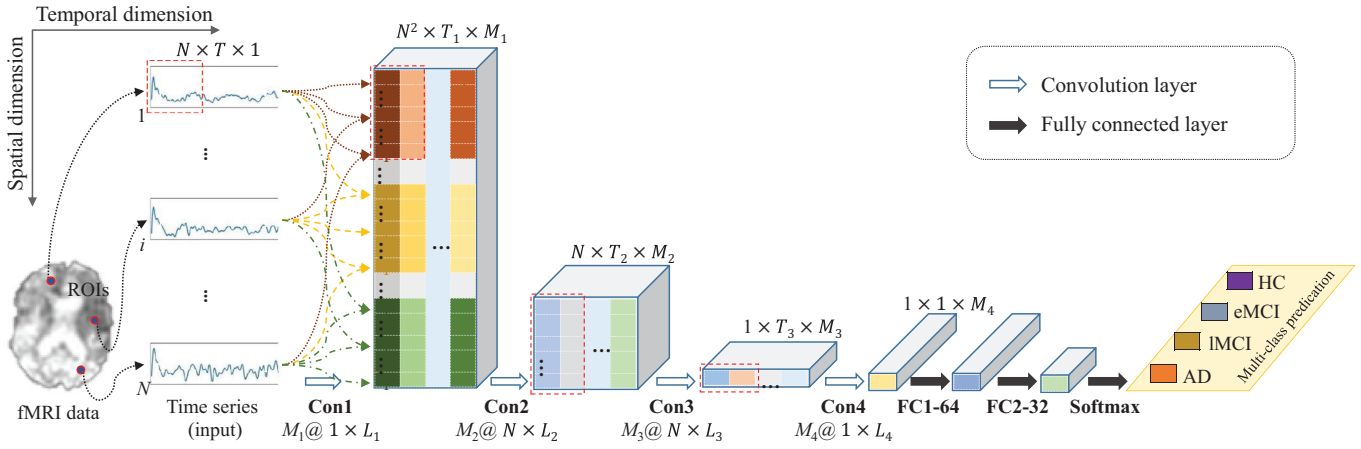

Fig. 1. Architecture of the proposed wck-CNN framework for dynamic FCN construction and analysis using fMRI data. There are four convolutional layers, *i.e.*, con1: connectivity construction layer, con2: regional feature extraction layer, con3: brain-network feature extraction layer and con4: temporal feature extraction layer, and two fully connected layers (*i.e.*, FC1 and FC2) including 64 and 32 units, respectively. Here, the kernel sizes in four layers are $1 \times L_1$, $N \times L_2$, $N \times L_3$ and $1 \times L_4$ (with the corresponding kernel numbers of M_1, M_2, M_3, M_4), respectively. T_1, T_2 and T_3 denote the total operations of using kernel along temporal dimension for con1, con2 and con3 layers, respectively. T is the length of time series of each ROI, and N is the number of ROIs.

In these previous studies, the FCNs are usually constructed by simply calculating the Pearson correlation coefficients (PCCs) between time series from brain regions, and then the low-level measures (*e.g.*, clustering coefficients) are extracted from the constructed FCNs as features to train a diagnostic model (*e.g.*, support vector machine, SVM). However, these studies have several critical limitations. *First*, during the construction of FCNs, they neglect the valuable observation information (*e.g.*, specific contributions of different time points). Intuitively, different time points could have different contributions for characterizing interactions among brain regions. In fact, studies have demonstrated that the functional connectivity calculated at specific time points can extend the usual pairwise interaction measures both in information and interpretability (Tagliazucchi et al., 2012; 2011). *Second*, the high-level and high-order network features that could further improve the performance are also neglected by these previous studies in feature extraction step. In addition, since network construction, feature extraction and classification are separately performed, it could yield sub-optimal learning model, thus degrading the diagnosis performance.

To address these problems and motivated by recent successful applications of convolutional neural networks (CNNs) in the natural image analysis field, in this paper we first define a weighted correlation kernel (called wc-kernel) for calculating the correlation between brain regions by using learned weights to characterize the contributions of different time points. Compared with previous methods (*e.g.*, PCC), our proposed wc-kernel can capture the specific contributions of different time points, thus conveying richer interaction information among brain regions. Furthermore, we build a wc-kernel based CNN (called wck-CNN) for constructing FCNs and extracting the hierarchical (*i.e.*, from local and global, and also from low-level to high-level) high-order features for brain disease classification, using fMRI data. Fig. 1 shows the architecture of our proposed wck-CNN method. Specifically, we first define a layer to build dynamic FCNs using our proposed wc-kernels. Here, we build multiple dynamic FCNs using multiple wc-kernels, with each one reflecting temporal changes of FCNs, thus conveying richer dynamic information of brain network. Then, we build another three layers to sequentially extract local (brain region specific), global (brain network specific), and temporal high-level and high-order features from the constructed low-level and low-order functional connectivities for classification. We evaluate the proposed wck-CNN method on 174 subjects (a total of 563 scans) with rs-fMRI data from the Alzheimer's Disease Neuroimaging Initiative (ADNI) database, [2] which includes 48 healthy controls (HC), 50 early MCI (eMCI), 45 late MCI (lMCI) and 31 AD. The experimental results suggest that our proposed method can *not only* improve the diagnostic performance compared with state-of-the-art methods, *but also* provide novel insights into the interaction patterns of brain activities and their changes in diseases.

The main contributions of this paper are four-fold. *First*, we define a wc-kernel to measure the correlation of brain regions, with weights learned in a data-driven manner to characterize specific contributions of different time points. The proposed wc-kernel is different from previous methods (*e.g.*, PCC method) that equally treat all time points. *Second*, we build a unified wck-CNN framework for defining FCNs and extracting hierarchical connectivities for disease diagnosis based on rs-fMRI data. To the best of our knowledge, this is among the first attempt to define the correlation kernel in CNN for characterizing the interactions among brain regions, and to build a unified CNN framework for dynamic FCN construction and analysis using fMRI data. *Third*, we provide an implementation for performing inference on brain network data. *Finally*, we investigate the changing connectivity patterns in AD/MCI patients.

The rest of the paper is organized as follows. In Section 2, we briefly review the related studies. Then, we describe the data used in the experiments, and present our proposed method and learning framework in Section 3. In Section 4, we describe conducted experiments and present corresponding results. In Section 5, we present discussions regarding the experiments and results. Finally, we conclude this paper in Section 6.

2. Related works

2.1. Functional connectivity network

FCNs that characterize the temporal correlation among blood oxygen level dependent (BOLD) signals of brain regions have shown great potential for understanding the functional activities of both healthy and abnormal human brains. Numerous

[2] http://adni.loni.usc.edu

studies have applied FCNs to analyzing brain diseases, including AD (Wang et al., 2013) and MCI (Bai et al., 2011), and reported a series of abnormal connectivity linked to specific brain regions, including hippocampus (Bai et al., 2009; Supekar et al., 2008), amygdala (Yao et al., 2013) and posterior cingulate cortex (Greicius et al., 2004). Also, studies in FCNs have found changes in network properties for patients with brain diseases, such as disrupted small world characteristics (characterized by high degree of clustering and short path length) in AD/MCI patients (Stam et al., 2007; Sanz-Arigita et al., 2010).

Conventional studies on the FCNs usually compute the correlation between brain regions over the whole scan period in rs-fMRI (Sporns, 2011), which implicitly assume that the functional connectivity is temporally stationary. However, recent studies demonstrate that the functional connectivity exhibits fluctuations over time (Catie Chang, 2010; Kiviniemi et al., 2011; Wang et al., 2019a), and thus a large number of studies have resorted to dynamic FCN to characterize the temporal changes of functional connectivity (Hutchison et al., 2013), and attempt to reveal the association between temporal changes in functional connectivity and brain diseases (Jones et al., 2012; Damaraju et al., 2014; Sakoğlu et al., 2010; Starck et al., 2013). For example, studies in (Jones et al., 2012; Wee et al., 2016; Zhang et al., 2018) have reported that rs-fMRI changes in AD/MCI patients extend beyond traditional (*i.e.*, stationary-based) FCNs.

Currently, studies on dynamic FCNs mainly focus on three aspects (*i.e.*, three levels): 1) temporal properties of functional connectivity between brain regions (Zalesky et al., 2014; Kucyi and Davis, 2014) (connectivity based level), 2) temporal variabilities of brain regions (Zhang et al., 2016; Jie et al., 2018) (region-based level), and 3) changing patterns of the whole network (Zhang et al., 2016) (network-based level). These studies suggest that the human brain is intrinsically organized into a dynamic interaction network (Fox et al., 2005; Sadaghiani and Kleinschmidt, 2013), demonstrating remarkable spatial-temporal variabilities in its function and structure (Sadaghiani and Kleinschmidt, 2013; Sadaghiani et al., 2010). Therefore, changing properties of dynamic FCNs may provide a critical cue for understanding the pathological underpinnings of brain diseases (Hutchison et al., 2013; Zhang et al., 2016; Wang et al., 2019b). However, measuring the changing properties of dynamic FCNs have been remaining as challenging tasks due to the complexity of the human brain (Hutchison et al., 2013; Preti et al., 2017).

On the other hand, these studies usually investigate the dynamics of FCNs using group analysis methods, this cannot be used for identifying patients with brain diseases from HCs at the individual level.

2.2. Connectivity-network-based classification

Recently, machine-learning-based methods have been applied to brain network analysis and automatic diagnosis of brain diseases (Arbabshirani et al., 2013; Guye et al., 2010; Jie et al., 2014a; Wee et al., 2014b). Connectivity-network-based learning methods typically include three main steps, *i.e.*, connectivity network construction, feature extraction and classifier construction.

2.2.1. Connectivity network construction

In the literature, a series of functional network construction methods have been proposed (see (Qiao et al., 2018; Smith et al., 2011) for a comprehensive review), including correlation-based methods (Sporns, 2011), graphical models (Bullmore et al., 2000; Friston et al., 2003), and sparse-learning-based methods (Wee et al., 2014a). Among them, correlation-based methods (*e.g.*, PCC) are the most commonly used, since they usually can obtain relatively high sensitivity for detecting network structures (Smith et al., 2011), and have been widely applied to the analysis of FCNs (Zhang et al., 2016; Sporns, 2011), including the AD/MCI classification (Seeley et al., 2009; Wee et al., 2012b). But, in the PCC method, all time points are assumed to contribute equally for computing the functional connectivity, thus ignoring the specific contributions of different time points. Intuitively, different time points could have different contributions for characterizing interactions between brain regions. Actually, existing studies have demonstrated that the resting brain spends most of the time near the critical time points (Tagliazucchi et al., 2012). Also, studies have shown that the functional connectivity constructed at some specific time points (*e.g.*, the time points with a relatively large amplitude BOLD fluctuation) can yield very important network properties (Tagliazucchi et al., 2011). Hence, considering the specific contributions of different time points could potentially provide further clues about the dynamic organization of resting state brain activity.

2.2.2. Feature extraction

Feature extraction aims to extract meaningful features from the constructed FCNs, followed by feature selection (*e.g.*, *t*-test and recursive feature elimination (RFE) Wee et al., 2011) to select the most discriminative feature subset for improving the learning performance. Among existing feature extraction methods, one simple approach is to extract/combine local network measures (*e.g.*, connectivity strengths, clustering coefficients, path lengths) as features for classification of brain diseases. For example, Chen et al. (2011) used connectivity strength features for AD/MCI classification. Wee et al. (2011) extracted clustering coefficient features from white matter networks for identification of MCI patients. Zanin et al. (2012) explored sixteen topological features from FCNs to classify the MCI patients from the HCs (healthy controls). One of the limitations for these studies is that they only extract local network features, thus ignoring global topological properties of networks. On the other hand, recent studies proposed more advanced method to learn global network features for brain disease classification (Jie et al., 2014b). Also, some studies attempt to integrate local and global network features for improving the classification performance of brain diseases (Jie et al., 2014a; Wen et al., 2018). All studies suggest the effectiveness of using local and global network features for brain disease diagnosis.

However, the major disadvantage of the existing methods is that they usually focus on the low-order network measures, thus neglecting high-order network features. Actually, studies in neuroscience have found significant high-order interactions in cortical activities (Ohiorhenuan et al., 2010; Yu et al., 2011), and recent studies also indicate that, compared with the low-order FCNs, the high-oder functional connectivity can convey more complex interactions (Chen et al., 2017). Hence, high-order network features could provide important information to help discover disease-related biomarkers to further improve the classification performance.

2.2.3. Classification

Based on features extracted from constructed brain networks, various classifiers, including support vector machine (SVM) (Wee et al., 2012b), logistic regression classifier (Uddin et al., 2013), and decision tree (Arbabshirani et al., 2013), have been used for identifing patients with brain diseases (*e.g.*, AD Chen et al., 2011, MCI Wee et al., 2012b and schizophrenia Sakoglu et al., 2009) from HCs. However, since the three key steps (*i.e.*, connectivity network construction, feature learning and classification) are separately performed in these methods, they could yield sub-optimal learning model, thus decreasing the classification performance.

Table 1
Characteristics of the studied subjects (Mean ± Standard deviation). MMSE: Mini-Mental State Examination.

Group	HC	eMCI	lMCI	AD
Male/Female	20/28	20/30	27/18	16/15
Age	76.0 ± 6.8	72.4 ± 7.1	72.3 ± 8.1	74.7 ± 7.4
MMSE	28.8 ± 1.4	28.1 ± 1.6	27.1 ± 2.1	21.8 ± 3.3
TR	3.00 ± 0.004	2.97 ± 0.148	3.00 ± 0.003	3.00 ± 0.001
Image resolution	3.29 ± 0.13	3.31 ± 0.04	3.28 ± 0.17	3.30 ± 0.08

2.3. Convolutional neural network

As powerful learning methods that can extract high-level, task-oriented features for prediction, deep learning approaches, *e.g.*, convolutional neural networks (CNNs), have been successfully applied to various tasks in medical image analysis, such as image segmentation (Dvorak and Menze, 2015; Zhu et al., 2017; Lian et al., 2018), image synthesis (Xiang et al., 2018; Pan et al., 2018; 2019), and brain disease diagnosis (Liu et al., 2017; 2018; Lian et al., 2019). However, deep learning models in these previous studies are usually trained over original MR images or original image patches rather than the connectivity networks. So far, few studies have applied deep learning methods to brain connectivity analysis. For example, Kawahara et al. (2016) recently built the first connectivity-network-oriented deep learning method for predicting cognitive and motor developmental outcome scores of preterm infants. Unfortunately, this method focuses on traditional FCNs, and thus cannot be used for dynamic FCN analysis. Another study (Henaff et al., 2015) explored to generalize convolutional operation to graph data, with graphs as input signals. However, since the FCNs are the fully-connected weighted graphs, these methods cannot be directly applied to FCN data.

To address the above-discussed problems, in this paper we first proposed a wc-kernel to measure the correlation between brain regions by using learned weights to characterize contributions of different time points. Then, we construct a unified CNN-based learning framework for constructing dynamic FCNs, learning hierarchical high-order features, and classifying patients from HCs, by using fMRI data. The experimental results on the ADNI dataset demonstrate the effectiveness of our proposed method.

3. Material and method

3.1. Subjects and fMRI data preprocessing

In this study, we use a total of 174 subjects with rs-fMRI data from ADNI database, including 48 HCs, 50 early MCI (eMCI), 45 late MCI (lMCI) and 31 AD. There, respectively, include 154, 165, 145, 99 scans for HC, eMCI, lMCI and AD subject groups, covering nine possible stages (*i.e.*, baseline, 6, 12, 24, 36, 48, 60, 72 and 84 months). There are 147 subjects with baseline scans, and other 27 subjects without baseline scan. Data acquisition is performed as follows: the image resolution is 2.29 − 3.31 mm for inplane and 3.31 mm slice thickness, TE=30 ms and TR=2.2 − 3.1 s. For each subject, there are 140 volumes. Table 1 presents the demographic and clinical information of these subjects. It is worth noting that the TR parameters are matched for eMCI vs. HC groups (with the p-value as 0.29) and AD vs. HC groups (with the p-value as 0.24). The image resolutions are also matched for both pairs of groups (with the corresponding p-values as 0.13 and 0.42, respectively). In addition, Table 2 illustrates the characteristics of scans of all subjects at nine stages. As one can observe, in most cases, samples in four categories (i.e., HC, eMCI, lMCI and AD) are generally balanced, while eMCI and AD have no samples at late stages (e.g., 48th month).

Table 2
Characteristics of scans of all 174 subjects at nine stages.

Scan stage	HC	eMCI	lMCI	AD
Baseline	37	42	37	31
6 m	29	38	30	24
12 m	31	40	27	18
24 m	37	40	29	21
36 m	6	5	8	5
48 m	2	0	2	0
60 m	4	0	4	0
72 m	6	0	5	0
84 m	2	0	3	0

Following Jie et al. (2018), image pre-processing is performed using a standard pipeline in FSL FEAT software package, [3] including removing the first 3 volumes, slice time correction, motion correction, bandpass filtering, and regression of white matter, CSF, and motion parameters. Since the head motion has substantial effects on FCN measures (Van Dijk et al., 2012), the scans with large head motion are discarded. That is, we have removed subjects with head motion more than 2.0 *mm* in any of direction or 2° in any of the rotation axis. The head motion profiles are matched for eMCI vs. HC groups (corresponding to p-value on mean motion equaling to 0.48) and AD vs. HC groups (corresponding to p-value equaling to 0.21). Structural skull stripping is performed using FSL, which is used to register the fMRI data to the Montreal Neurological Institute space. 6 mm Gaussian kernel is performed to smooth the fMRI data. The subjects with more than 2.5 min of large frame-wise displacement (FD > 0.5) are not included in this study (i.e., excluded before data inclusion). Here, we do not perform data scrubbing (*i.e.*, removing volumes with FD > 0.5) because it could introduce additional artifacts for the subsequent dynamic network analysis. The BOLD signals are band-pass filtered ($0.015 \leq f \leq 0.15$Hz). The brain space of fMRI scans is partitioned into the 116 regions of interest (ROIs) using the automated anatomical labeling (AAL) template (Tzourio-Mazoyer et al., 2002). Table S1 in the *Supporting Information* gives the IDs and names of 116 ROIs. For each subject, the mean time series are extracted from each ROI, and the time point signal of each ROI is normalized as following:

$$f(s) = (s - \mu_i)/\sigma_i \tag{1}$$

where s corresponds to the time point signal from the ith ROI, and μ_i and σ_i denote the mean and standard deviation of time series from the ith ROI, respectively.

3.2. Proposed weighted correlation kernel

To capture specific contributions of different time points, we define a wc-kernel for measuring the correlation between brain regions, *i.e.*,

$$k(\mathbf{x}_i, \mathbf{x}_j) = \sum_{l=1}^{L_1} \mathbf{w}^l \mathbf{x}_i^l \mathbf{x}_j^l \tag{2}$$

[3] http://fsl.fmrib.ox.ac.uk/fsl/fslwiki/FEAT

where $\mathbf{x}_i$ is the normalized (using Eq. (1)) time series from the ith ROI, $\mathbf{x}_i^t$ is the corresponding time point signal, $\mathbf{w} = [\mathbf{w}^1, \mathbf{w}^2, \ldots, \mathbf{w}^{L_1}]$ denotes a learnable weight vector, and the kernel size is $1 \times L_1$.

According to the definition in Eq. (2), our proposed wc-kernel calculates the correlation between a pair of ROIs by using a learnable weight vector $\mathbf{w}$ to characterize specific contributions of different time points. It is easy to show that our defined wc-kernel reduces to the PCC when all elements in $\mathbf{w}$ equal to 1. Therefore, our defined wc-kernel is actually an extension of the PCC, thus can convey richer interaction information of brain regions compared with the PCC method.

3.3. Architecture of the proposed wc-kernel based CNN

As shown in Fig. 1, our proposed wck-CNN framework contains four convolutional layers and two fully connected layers. A rectified linear unit (ReLU) is used as the activation function of each layer, and each fully connected layer is followed by dropout with a rate of 0.50 (Hinton et al., 2012). The input of our proposed wck-CNN method is time series from all ROIs, and the output (via softmax) is the probability of the subject belonging to each of four categories (*i.e.*, AD, lMCI, eMCI and HC). Here, M_1, M_2, M_3 and M_4 are the numbers of kernels in the four convolutional layers, respectively. In the following, we will present the details of the four convolutional layers.

3.3.1. Connectivity construction layer

We define the first convolutional layer (*i.e.*, connectivity construction layer) for constructing FCNs using our defined wc-kernels, with time series of ROIs as the input. Given a wc-kernel k defined in Eq. (2), the output of this layer is a matrix $\mathbf{C} \in R^{N^2 \times T_1}$ with

$$\mathbf{C}_{(i-1)\times N+j,t} = k(\S_i^t, \S_j^t) \tag{3}$$

where $\S_i \in R^T$ denotes the whole time series of the ith ROI, $\S_i^t$ corresponds to segment of time series when performing the tth operation of sliding kernel along the temporal dimension (corresponding to time series of ROIs), T_1 is the total operations of sliding kernel along the temporal dimension, T is the length of time series, and N is the number of ROIs.

According to Eq. (3), the convolutional operation along the spatial dimension (corresponding to any pair of ROIs) calculates functional connectivity between a pair of ROIs, reflecting their interactions. And, the FCN (*i.e.*, matrix) is concatenated into a vector represented as one column in $\mathbf{C}$. For example, $\mathbf{C}_{(i-1)\times N+j-1,t}$ denotes the functional connectivity between ROIs i and j with performing the tth operation of sliding kernel along the temporal dimension. Meanwhile, the convolutional operation along the temporal dimension calculates different functional connectivities of the same pair of ROIs within different segments of time series, which is similar to the sliding window method in the conventional dynamic FCN construction, reflecting temporal dynamics of functional connectivity. Thus, the matrix $\mathbf{C}$ represents a set of FCNs, which characterizes the dynamics of FCNs, reflecting both spatial and temporal changes of functional connectivity. Finally, the output of this layer with M_1 wc-kernels is a $3D$ tensor, which contains M_1 dynamic FCNs, conveying richer dynamics of brain networks.

3.3.2. Regional feature extraction layer

To extract region-specific features, we define a regional feature extraction layer using the dynamic FCNs produced by the connectivity construction layer as the input data. Specifically, we set the size of kernels to $N \times L_2$, and set the stride along both dimensions (*i.e.*, temporal and spatial dimensions) to (N, 1).

In regional feature extraction layer, the convolution along the spatial dimension is a feature mapping for each ROI, which can be interpreted as calculating a single output value for each ROI i by computing the weighted combination of functional connectivity connected to ROI i across L_2 (> 1) neighboring FCNs. The convolution along the temporal dimension corresponds to different feature mappings of the same ROI, reflecting temporal changes of each specific ROI. It should be emphasized that, since the features extracted in this layer are calculated based on series of functional connectivities of specific ROI across multiple FCNs, there feature are high-order, and characterize temporal variability of brain regions.

3.3.3. Brain-network feature extraction layer

Following the regional feature extraction layer, we build a brain-network feature extraction layer to learn the brain-network-specific features, with the regional feature representations as the inputs. Specifically, we set the size of kernels is $N \times L_3$, and set the size of stride along both dimensions to (1, 1).

In this layer, the convolution along the spatial dimension is a feature mapping for the whole FCN, which can be interpreted as calculating a single output value for whole FCN by computing the weighted combination of all region-specific features across L_3 (> 1) neighboring time points. The convolution along the temporal dimension corresponds to different mappings for the whole FCN, characterizing the temporal properties of the brain network. Similar to the regional feature extraction layer, the features extracted in this layer are also high-order.

3.3.4. Temporal feature extraction layer

To reduce the feature dimensionality and thus decrease the complexity of learned model, we further build a temporal feature extraction layer to learn temporal feature of the whole FCN. Specifically, we set the size of kernels is $1 \times L_4$, set the size of stride along both dimensions to (1, 1), and perform an average-pooling (AP) operation after convolution to map all features into a feature. Therefore, the output of this layer with a learned kernel can be interpreted as a measure for the temporal variability of the whole dynamic FCN.

It is worth noting that in the proposed wck-CNN method, the first convolution layer (*i.e.*, connectivity construction layer) is used for constructing dynamic FCNs (*i.e.*, sets of FCNs), which characterizes the dynamics of FCNs. The last three convolution layers (*i.e.*, regional feature extraction layer, brain-network feature extraction layer and temporal feature extraction layer) are used for extracting the high-level and high-order network dynamic features from constructed FCN sets for subsequence classification.

4. Experiments and results

4.1. Experimental settings

We perform two groups of experiments, including 1) two binary classification tasks, *i.e.*, eMCI vs. HC and AD vs. HC classifications, 2) a multi-class classification task, *i.e.*, AD vs. lMCI vs. eMCI vs. HC classification, by using a 5-fold cross-validation. Specifically, for each classification task, the set of subjects with baseline scan is (roughly) equivalently partitioned into five subsets. One subset is used as the testing set. The remaining four subsets and subjects without baseline scan are combined to construct the training set. In addition, in each cross validation we select 15% training subjects as the validation data for tuning the parameters. It is worth noting that, to enhance the generalization ability of our model, all scans of each training subject are used as training data, with each scan as an independent sample but with the same class

Table 3
Performance of all methods in two binary classification tasks, *i.e.*, eMCI vs. HC and AD vs. HC classifications. ACC= Accuracy.

Method	eMCI vs. HC (%)			AD vs. HC (%)		
	ACC	ACC_{HC}	ACC_{eMCI}	ACC	ACC_{HC}	ACC_{AD}
Baseline	57.1	48.1	65.6	73.3	77.8	66.7
SVM	63.6	50.0	75.0	75.0	80.0	66.7
CNN	72.0	68.7	74.8	76.4	76.7	77.8
DFCN-CNN	74.8	63.3	84.5	78.3	78.0	80.0
wck-CNN-1	81.8	***90.0***	75.0	85.8	82.5	***91.7***
wck-CNN	***84.6***	83.3	***85.7***	***88.0***	***87.8***	88.9

Table 4
Performance of all methods in the multi-class classification task, *i.e.*, AD vs. lMCI vs. eMCI vs. HC classification. ACC= Accuracy.

Method	AD vs. lMCI vs. eMCI vs. HC (%)				
	ACC	ACC_{HC}	ACC_{eMCI}	ACC_{lMCI}	ACC_{AD}
Baseline	30.6	20.0	38.9	30.0	33.3
SVM	35.0	22.0	69.5	21.0	6.7
CNN	44.2	32.2	***74.6***	28.3	22.2
DFCN-CNN	50.0	38.3	53.0	53.8	***58.3***
wck-CNN-1	54.5	52.2	62.7	45.0	55.6
wck-CNN	***57.0***	***68.9***	52.4	***56.7***	44.4

label. We evaluate the performance by computing the overall accuracy of all categories, and the accuracy for each category. In the experiment, we set the parameters as followings: $T = 137$, $T_1 = 34$, $T_2 = 33$, $T_3 = 32$, $M_1 = 16$, $M_2 = 32$, $M_3 = 64$, $M_4 = 64$, $L_1 = 70$, $L_2 = 2$, $L_3 = 2$ and $L_4 = 8$. In connectivity construction layer, we set the size of stride along temporal dimension to 2. Notably, other scans (excepting for the baseline) of the testing subjects are not selected as training data or testing data.

4.2. Methods for comparison

We first compare the proposed method with traditional FCN based on the SVM method (denoted as **SVM**). Specifically, in the SVM method, the FCN of each subject is first built by computing the PCC between the whole time series of a pair of ROIs. The local clustering coefficients of all 116 ROIs are then extracted from constructed FCNs as features. A *t*-test method with the threshold (*i.e.*, $p-$value < 0.05) is used for feature selection, followed by a linear SVM with default parameters for classification. Besides, we also compare with the **baseline** method using the connectivity strengths from traditional FCNs as features, where *t*-test and a linear SVM with default parameters are also used for feature selection and classification, respectively. Here, a one-to-all strategy is used for multi-class classification task.

To evaluate the contributions of a series of essential components used in the proposed method, we compare wck-CNN with its three variants. These variants include 1) CNN method using traditional FCNs (denoted as **CNN**), 2) CNN method using dynamic FCNs (denoted as **DFCN-CNN**), and 3) wck-CNN method without using high-order feature information (denoted as **wck-CNN-1**). The CNN and DFCN-CNN methods are implemented to contain the Con2, Con3, Con4 and two fully connected layers (without our proposed wc-kernel based network construction layer), while using the traditional FCNs and dynamic FCNs as input layers, respectively. Here, following Wee et al. (2016), the FCNs and dynamic FCNs are built by computing the PCC between the time series of ROIs, and the dynamic FCNs are constructed using an overlapping sliding window method with the window length equal to 70, and the translation step equal to 2. These methods have the same parameters as our proposed wck-CNN method excepting for setting $M_1 = 1$ in both methods (*i.e.*, CNN and DFCN-CNN) and $T_1 = T_2 = T_3 = 1$ in the CNN method. In wck-CNN-1 method, no high-order features are extracted in regional feature extraction layer and brain-network feature extraction layer, *i.e.*, $L_1 = 1$ and $L_2 = 1$.

4.3. Classification performance

Tables 3 and 4 summary the results of all methods for two binary classification tasks and the multi-class classification task, respectively. As can be seen from Tables 3 and 4, our proposed wck-CNN method outperforms the competing methods in all the three classification tasks. For instance, our proposed wck-CNN method yields the accuracy of 84.6% and 88.0% for eMCI vs. HC classification and AD vs. HC classification, respectively, while the best accuracies obtained by the competing methods are 74.8% and 78.3%, respectively (where wck-CNN-1 is still a variant of our proposed method). For AD vs. lMCI vs. eMCI vs. HC classification, our proposed wck-CNN method achieves the overall accuracy of 57.0%, while the best overall accuracy of the competing methods is 50.0%. These results suggest the effectiveness of our proposed wck-CNN method for brain disease diagnosis.

In addition, from Tables 3 and 4, we can summarize another four interesting observations. *First*, the wc-kernel based methods (*i.e.*, wck-CNN-1 and wck-CNN) perform better than the conventional PCC based method (*i.e.*, baseline, SVM, CNN and DFCN-CNN), indicating the effectiveness of our defined wc-kernel in conveying the interaction information among brain regions. *Second*, the wck-CNN method can achieve higher performance in comparison with wck-CNN-1 method, demonstrating the advantage of exploring high-order information from connectivity networks. *Third*, compared with traditional learning methods (*i.e.*, baseline and SVM), CNN-based methods (*i.e.*, CNN, DFCN-CNN wck-CNN-1 and wck-CNN) can achieve much higher performance, suggesting that CNN can capture the underlying properties of brain networks, and thus can be better applied for brain network analysis. *Finally*, compared with traditional FCN-based methods (*i.e.*, baseline, SVM and CNN), dynamic FCN based methods (*i.e.*, DFCN-CNN, wck-CNN-1 and wck-CNN) can achieve higher accuracies, indicating that the dynamics of FCNs can provide useful information for better understanding the pathology of brain diseases, which is consistent with results reported in the existing studies (Hutchison et al., 2013; Jones et al., 2012; Wee et al., 2016).

On the other hand, Fig. 2 presents the total loss on the training subjects and validation subjects in each fold of cross validation for AD vs. lMCI vs. eMCI vs. HC classification task. From Fig. 2, we can see that our proposed wck-CNN method can converge fast within 40 epoch.

4.4. Connectivity analysis

Furthermore, we investigate the connectivity constructed by our proposed wck-CNN method. Specifically, we first construct the dynamic FCNs (*i.e.*, the output of connectivity construction layer in our proposed wck-CNN method) for all subjects using the wc-kernels learned in the first fold cross-validation of AD vs. lMCI vs. eMCI vs. HC classification task. Figure S1 in the *Supporting Information* plots the weight values of these 16 wc-kernels. We can obtain 16 dynamic FCNs (*i.e.*, 16 sets of FCNs) for each subject with 16 wc-kernels. For simplicity, we calculate the average brain network for each dynamic FCN (*i.e.*, set of FCNs) of each subject. Thus, we obtained 16 average brain networks with 16 dynamic FCNs for all subjects. Then, we test the group difference of functional connectivity in each average brain network using the standard *t*-test. Fig. 3 reports the obtained results on 16 average brain networks (denoted as wck1 to wck16) for (a) eMCI vs. HC groups, and (b) AD vs. HC groups. For comparison, Fig. 3 also reports the

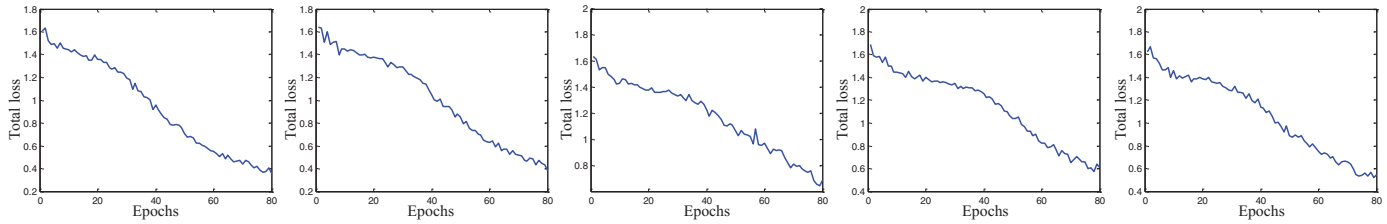

(a) Total loss on the training subjects

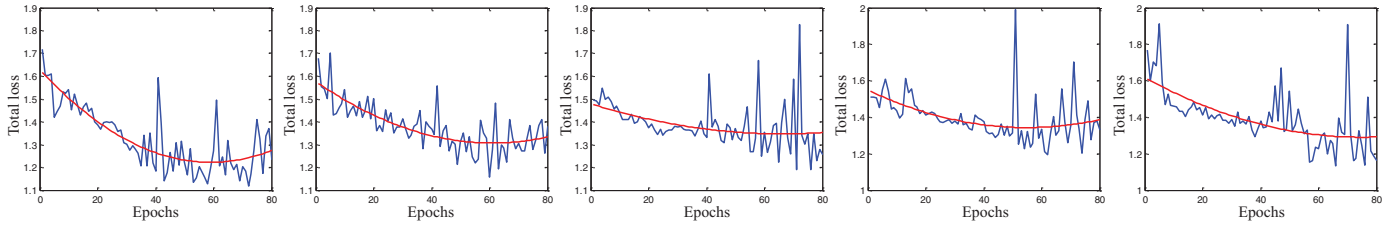

(b) Total loss on the validation subjects

Fig. 2. Total loss of the proposed wck-CNN method with 80 epochs in each fold cross-validation (from left to right) for AD vs. lMCI vs. eMCI and NC classification task. Here, (a) total loss on the training subjects, and (b) total loss on the validation subjects.

group difference of functional connectivity in the traditional FCNs and dynamic FCNs constructed by the overlapping sliding windows method. Here, we set p-values more than 0.05 to 1 for clarity.

From Fig. 3, we can make three interesting observations for most of average brain networks, compared with the traditional FCNs and dynamic FCNs. *First*, there are more discriminative functional connectivity (with the corresponding p-value less than 0.05) on both eMCI vs. HC groups and AD vs. HC groups, suggesting that our proposed wc-kernel based dynamic FCNs are more discriminative. *Second*, there are more obvious patterns. For instance, the discriminative functional connectivity between AD and HC groups focus on connections with specific brain regions, including lateral surface, parietal lobe, limbic lobe and sub cortical gray nuclei, which have been widely reported in the previous studies. Table 5 demonstrates these specific brain regions that have significant differences of function connectivity for two group pairs (*i.e.*, eMCI vs. HC groups and AD vs. HC groups). *Finally*, there contain few discriminative functional connectivity between brain regions within the cerebellum, but have some discriminative functional connectivity between the cerebellum and the cerebrum, suggesting that the cerebellum might be related with AD/MCI and it may provide useful information for disease prognosis (Baldaçara et al., 2011; Weis et al., 2004).

From Fig. 3, Table 5, we can see that, compared with HC group, some functional connectivity on specific brain regions, such as middle cingulate gyrus, posterior cingulate gyrus, inferior parietal lobule, supramarginal gyrus and paracentral lobule, are all significantly changed for the eMCI group and the AD group, indicating that those brain regions may be much related to the early stage of AD. Besides, there are more discriminative functional connectivity and more brain regions with significant differences of functional connectivity for the AD subjects compared with the eMCI subjects. This implies that, with the disease progress, more functional connectivity and brain regions are affected by the AD.

To further visualize the differences of connectivity networks for different groups, we construct an average connectivity network for each group (*i.e.*, AD, eMCI and HC groups). Specifically, following the step of average brain network construction in the 1st paragraph of this subsection, we also compute the 16 dynamic FCNs using 16 wc-kernels learned in the first fold cross-validation of AD vs. lMCI vs. eMCI vs. HC classification task, and then compute a total average connectivity network for all 16 dynamic FCNs of subjects in each group. Finally, we compute the difference of average connectivity networks between these groups. Fig. 4 plots the difference in average connectivity strength of the ROIs from Table 5 between two pairs of groups (*i.e.*, eMCI vs. HC groups, and AD vs. HC groups). Here, the color represents the corresponding difference value. From Fig. 4, we can observe significant reductions in connectivity strengths for the eMCI/AD groups compared with the NC group, indicating possible disruptions in connectivity between these brain regions, as reported in the existing studies (Wang et al., 2013; Bai et al., 2011; Supekar et al., 2008; Yao et al., 2013). In addition, as can be seen from Fig. 4, the changes in connectivity strengths are more significant for the AD subjects compared with the eMCI subjects, indicating that the damage of AD on the brain function is gradually enhanced along the disease progress.

In order to evaluate the generalization of the proposed method, we further test the group difference of functional connectivity in average brain networks of testing subjects in the first fold cross-validation of AD vs. lMCI vs. eMCI vs. HC classification task. Figure S2 in the *Supporting Information* gives the obtained results. For comparison, Figure S2 also gives the group difference of functional connectivity in the traditional FCNs and dynamic FCNs of these testing subjects. As can be seen from Fig. S2, the proposed wc-kernel based dynamic FCNs are also more discriminative on both eMCI vs. HC groups and AD vs. HC groups, *i.e.*, there still includes more discriminative functional connectivity (with corresponding p-value less than 0.05) for most of average brain networks in comparison with those of traditional FCNs and dynamic FCNs, indicating the efficacy of our proposed method.

4.5. Discriminative power of learned features

In this section, we investigate the discriminative power of features learned in our proposed wck-CNN method. Specifically, we first extract 64 features (corresponding to the output of temporal feature layer in our proposed wck-CNN method) of all subjects by using the learning model in the first fold cross-validation of the four-class classification task. It worth noting that each of the 64 features can be treated as a measure of network properties, which

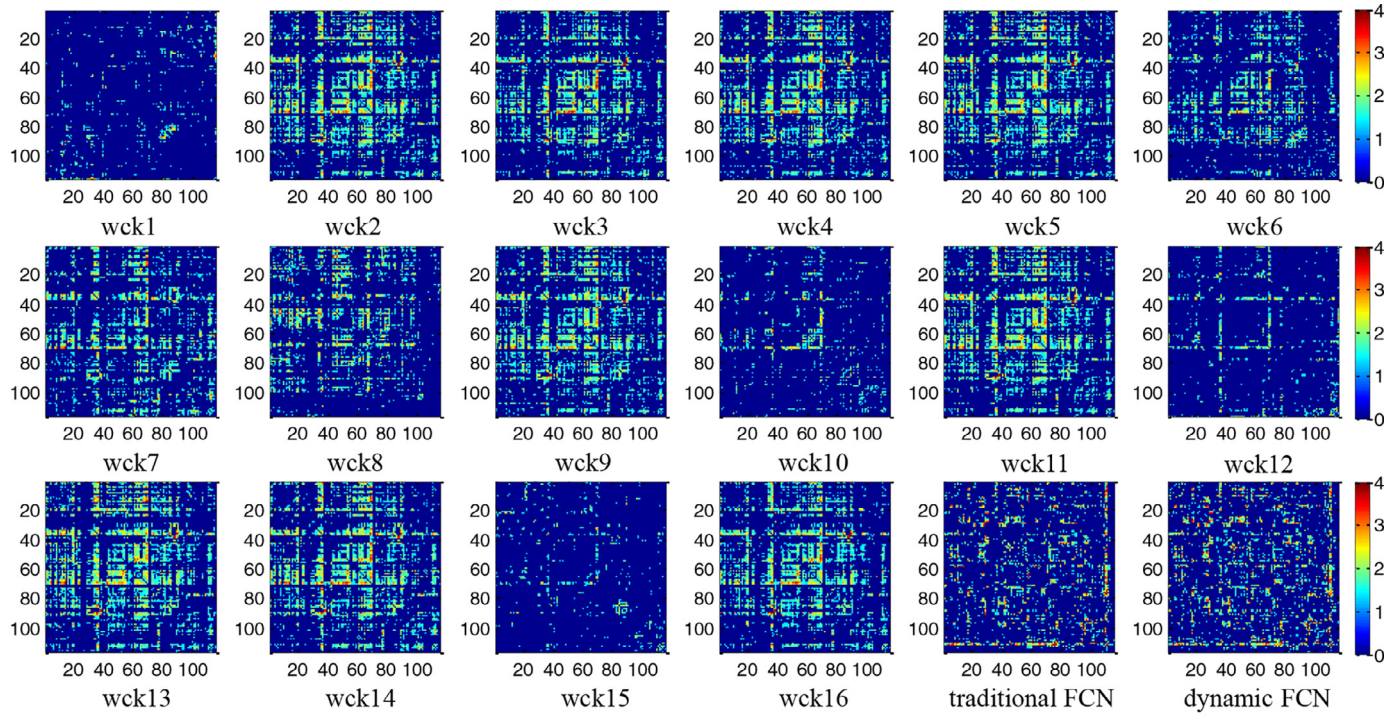

(a) **eMCI vs. HC groups**

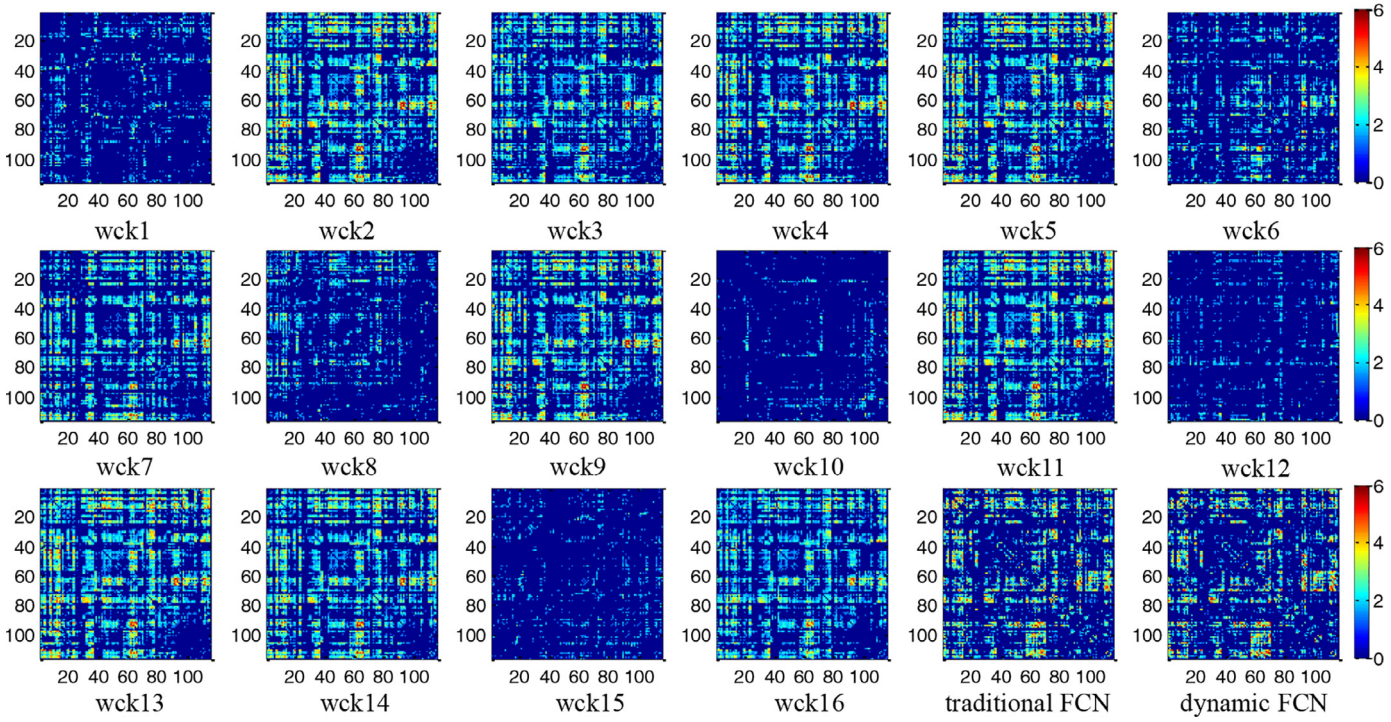

(b) **AD vs. HC groups**

Fig. 3. Group difference of functional connectivity constructed using different methods for (a) eMCI vs. HC groups, and (b) AD vs. HC groups. Here, p-values more than 0.05 are set to 1, colors in (a) and (b) denote the value of $-\log 10(p\text{-value})$, and {wck1,..., wck16} correspond to the dynamic FCNs constructed by using the proposed method with 16 different wc-kernels, respectively. Dynamic FCN is constructed by using the overlapping sliding windows method. See Table S1 in the *Supporting Information* for the names of these 116 ROIs.

Table 5
Important brain regions with significant difference of functional connectivity for (left) eMCI vs. HC groups, and (right) AD vs. HC groups.

eMCI vs. HC groups		AD vs. HC groups	
Name	Abbr.	Name	Abbr.
Suplementary motor area left	L.SMA	Superior frontal gyrus (dorsal) left	L.SFGdor
Suplementary motor area right	R.SMA	Superior frontal gyrus (dorsal) right	R.SFGdor
Middle cingulate gyrus left	L.MCG	Middle frontal gyrus left	L.MFG
Middle cingulate gyrus right	R.MCG	Middle frontal gyrus right	R.MFG
Posterior cingulate gyrus left	L.PCG	Inferior frontal gyrus (opercular) left	L.IFGoperc
Posterior cingulate gyrus right	R.PCG	Inferior frontal gyrus (opercular) right	R.IFGoperc
Inferior occipital gyrus left	L.IOG	Inferior frontal gyrus (triangular) left	L.IFGtriang
Inferior parietal lobule left	L.IPL	Inferior frontal gyrus (triangular) right	R.IFGtriang
Supramarginal gyrus left	L.SMG	Superior frontal gyrus (media) left	L.SFGmed
Precuneus left	L.PCUN	Superior frontal gyrus (media) right	R.SFGmed
Precuneus right	R.PCUN	Middle cingulate gyrus left	L.MCG
Paracentral lobule left	L.PCL	Middle cingulate gyrus right	R.MCG
Paracentral lobule right	R.PCL	Posterior cingulate gyrus left	L.PCG
Middle temporal gyrus left	L.MTG	Posterior cingulate gyrus right	R.PCG
Inferior temporal right	R.ITG	Inferior parietal lobule left	L.IPL
		Inferior parietal lobule right	R.IPL
		Supramarginal gyrus left	L.SMG
		Supramarginal gyrus right	R.SMG
		Angular gyrus right	R.ANG
		Paracentral lobule right	R.PCL
		Pallidum left	L.PAL
		Pallidum right	R.PAL
		Thalamus left	L.THA
		Thalamus right	R.THA
		Superior temporal gyrus right	R.STG

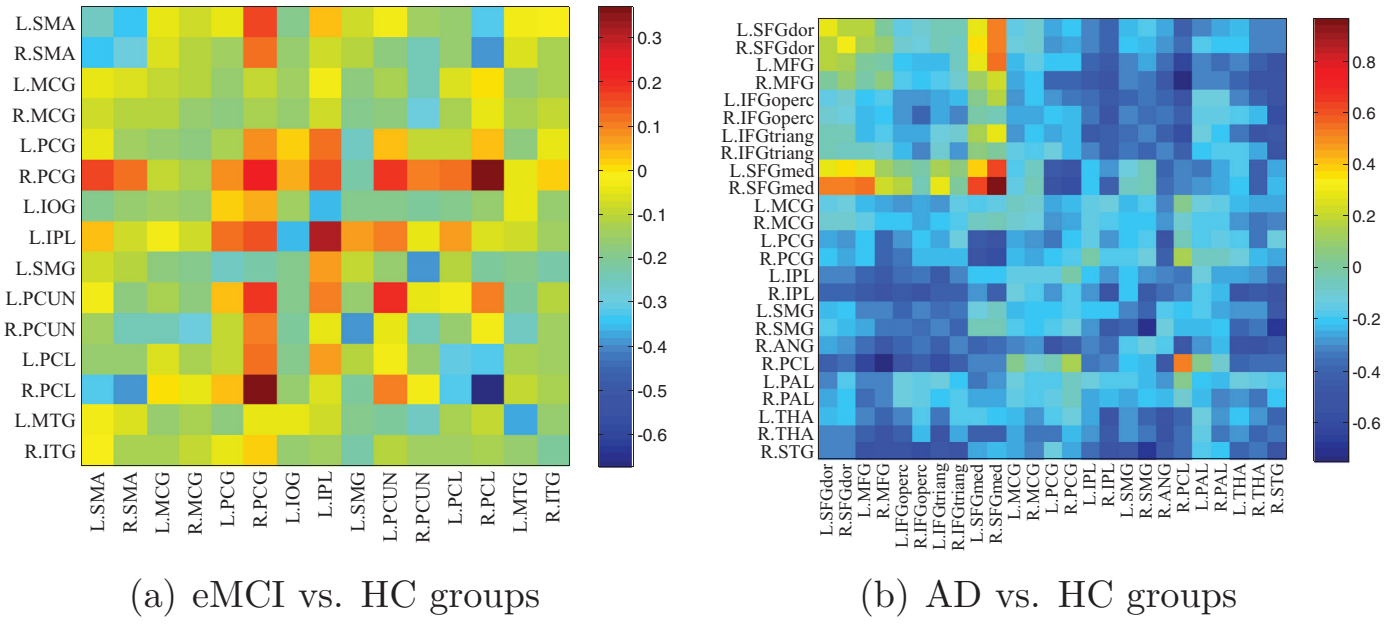

(a) eMCI vs. HC groups (b) AD vs. HC groups

Fig. 4. The difference in average connectivity strength for (a) eMCI vs. HC groups, (b) AD vs. HC groups.

reflects the temporal properties of dynamic FCNs. Then, we calculate the discriminative power of all 64 features in both group pairs (*i.e.*, eMCI vs. HC groups, and AD vs. HC groups), using the standard *t*-test. Figs. 5 and 6 plot the obtained *p*-values for both group pairs, respectively. For comparison, in Figs. 5 and 6 we give the discriminative power of features learned by the compared methods (*i.e.*, baseline, SVM, CNN, DFCN-CNN and wck-CNN-1). It is worth noting that there are all 6670 connectivity strength features in baseline method and 116 clustering coefficient features in the SVM method, while, there are 64 features in all CNN-based methods (*i.e.*, CNN, DFCN-CNN, wck-CNN-1 and wck-CNN). In addition, Table 6 gives the average and median of the *p*-value for all features in both group pairs.

As can be seen from Figs. 5 to 6 and Table 6, most of the features learned in our proposed wck-CNN method have *p*-values smaller than 0.001, suggesting good discriminative power between patients and HCs. In addition, the features learned by our wck-CNN are more discriminative than the features learned by the competing methods. This validates the effectiveness of our proposed wck-CNN method for learning the network features, and also partly explains why our proposed wck-CNN method can yield better classification performance compared with the competing methods.

Moreover, we feed the features learned by wck-CNN to SVM for classification, to further study the discriminative power of these features. Specifically, we first calculate 64 learning features for all subjects by using the learning model obtained in one of 5-fold

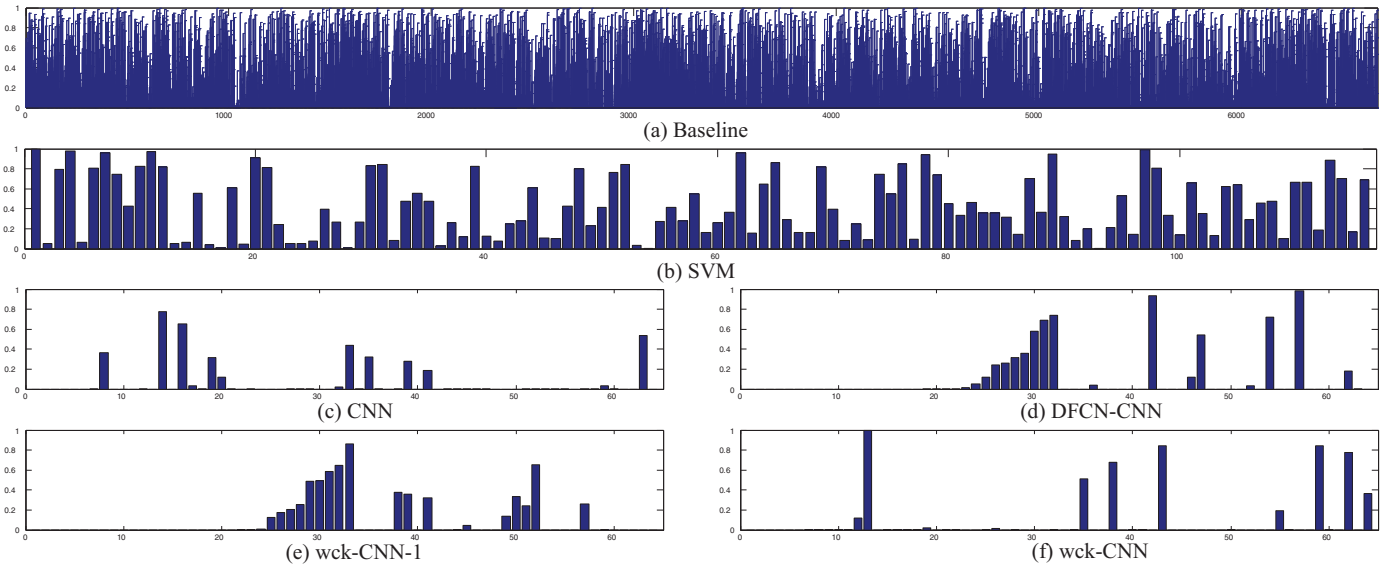

Fig. 5. The discriminative power of learning features between eMCI and HC groups for all methods (*i.e.*, (a) baseline, (b) SVM, (c) CNN, (d) DFCN-CNN, (e) wck-CNN-1 and (f) wck-CNN).

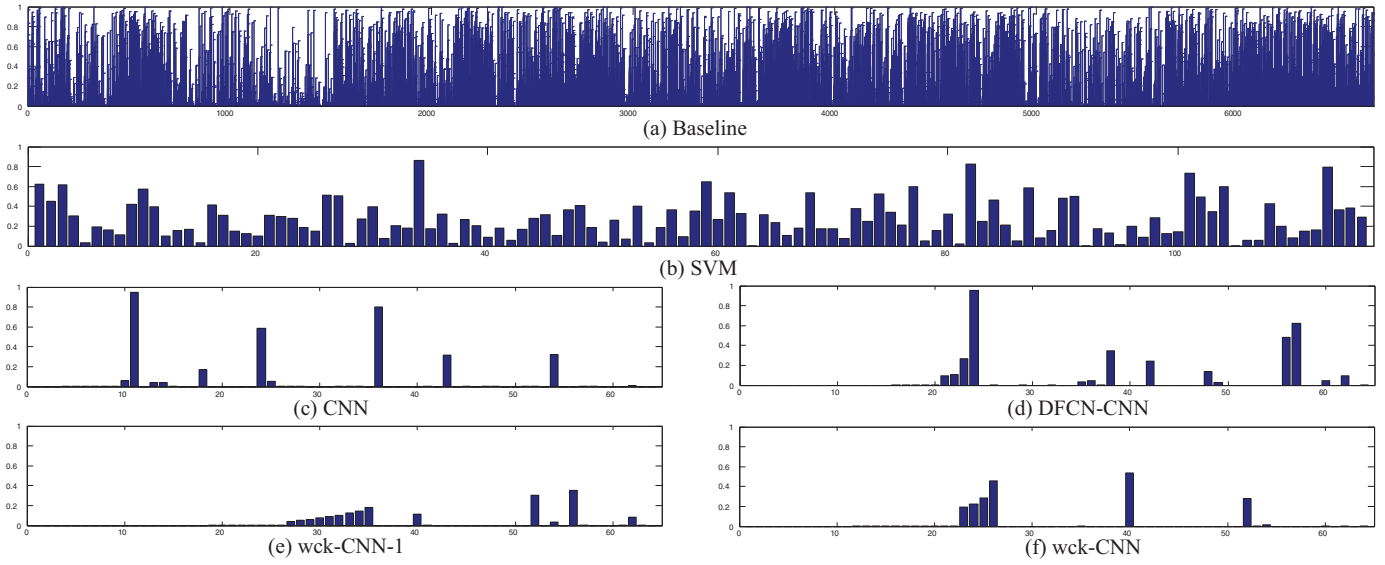

Fig. 6. The discriminative power of learning features between AD and HC groups for all methods (*i.e.*, (a) baseline, (b) SVM, (c) CNN, (d) DFCN-CNN, (e) wck-CNN-1 and (f) wck-CNN).

Table 6
The average and median of p-value for learning features in both group pairs (*i.e.*, eMCI vs. HC groups, and AD vs. HC groups.

Method	eMCI vs. HC		AD vs. HC	
	Mean	Median	Mean	Median
Baseline	0.36	0.29	0.29	0.17
SVM	0.43	0.36	0.27	0.21
CNN	0.06	$< 1E-6$	0.05	$< 1E-6$
DFCN-CNN	0.11	$< 1E-6$	0.06	$< 1E-6$
wck-CNN-1	0.10	$< 1E-6$	0.03	$< 1E-6$
wck-CNN	0.08	$< 1E-6$	0.03	$< 1E-6$

Table 7
The total accuracy of all methods using features learned in three classification task (%).

Method	eMCI vs. HC	AD vs. HC	AD vs. lMCI vs. eMCI vs. HC
Baseline	55.8	66.7	24.6
SVM	61.0	72.9	25.4
CNN	74.1	75.8	48.5
DFCN-CNN	74.1	76.4	52.5
wck-CNN-1	80.8	81.6	55.2
wck-CNN	81.1	85.3	57.6

cross-validations. Then, we train a linear SVM (with default parameters) using the learned features for the training subjects, and apply the trained SVM to the testing subjects. Table 7 reports the obtained average accuracy in all 5-fold cross-validations for three classification tasks of eMCI vs. HC, AD vs. HC, and AD vs. lMCI vs. eMCI vs. HC. For comparison, Table 7 also shows the classification accuracy of features learned by the competing methods using traditional SVM classifier. It is worth noting that no feature selection method is performed in all methods (*i.e.*, all learned features are used for training model and classification).

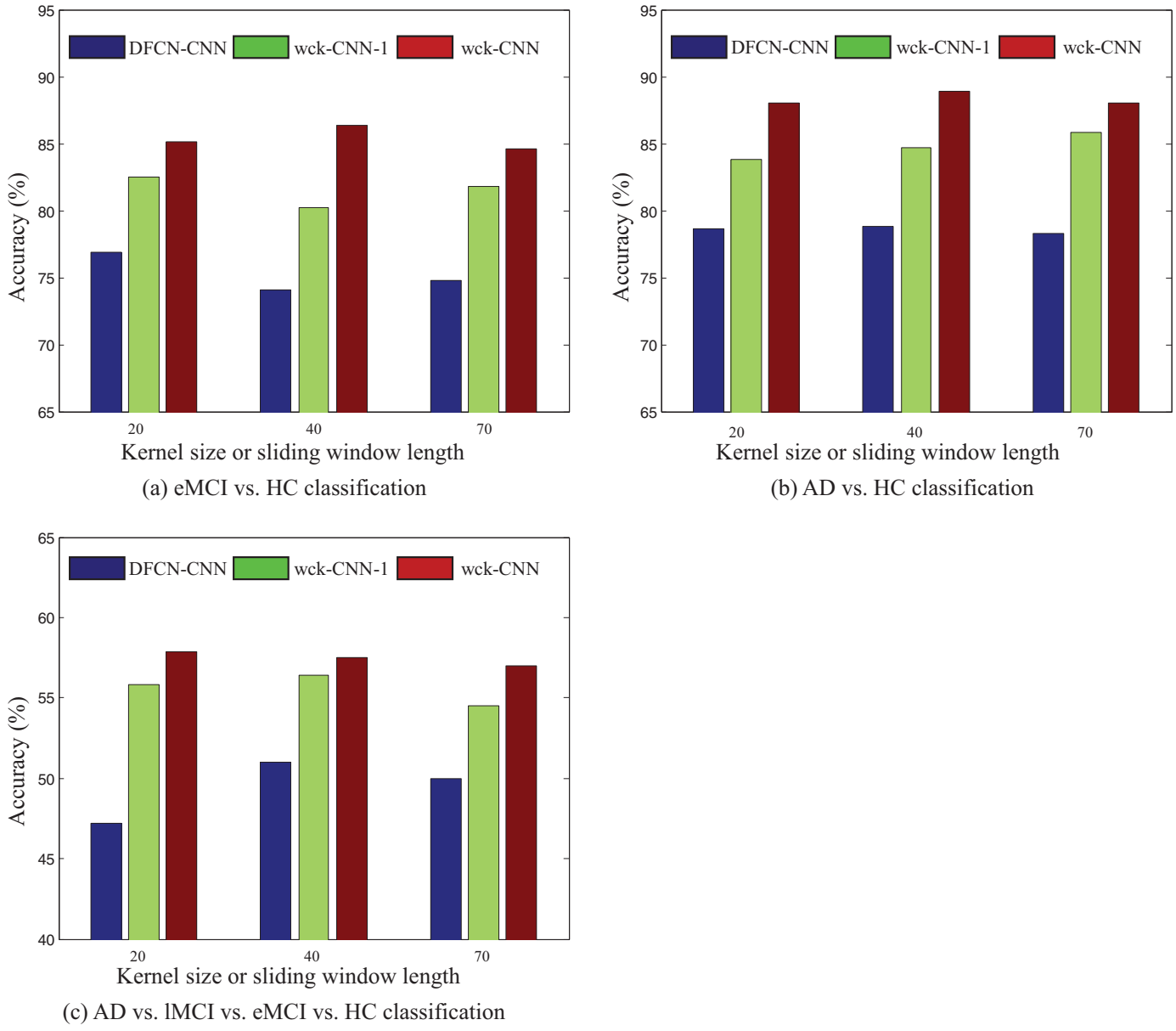

Fig. 7. The classification accuracy of dynamic FCN based methods (*i.e.*, DFCN-CNN, wck-CNN-1 and wck-CNN) *w.r.t.* different kernel sizes or sliding window lengths on tasks of (a) the eMCI vs. HC classification, (b) the AD vs. HC classification, and (c) the AD vs. lMCI vs. eMCI vs. HC classification.

As we can see from Table 7, the features learned by our proposed wck-CNN method can yield better classification accuracy that the features generated by the competing methods. These results further indicate the discriminative power of our wck-CNN method.

5. Discussion

5.1. Significance of results

FCNs have been widely applied to diagnosing physiological and psychiatric disease, such as AD and MCI. To construct FCNs, the PCC method is usually used to measure the correlation among different brain regions (Aerts et al., 2016; Zhang et al., 2016; Córdova-Palomera et al., 2017). The main disadvantage of the PCC method is treating different time points equally, thus ignoring specific contributions of different time points. In this paper, we define a novel wc-kernel to measure the correlation among brain regions, learning different weights to characterize specific contributions of different time points. We then construct a unified wck-CNN framework for brain disease classification based on fMRI data. To the best of our knowledge, our proposed method is among the first attempt to define the correlation kernel for characterizing the interactions between brain regions, and to build a CNN framework for dynamic FCN analysis using fMRI data. The experimental results on 174 subjects from ADNI database show that our proposed wck-CNN method outperforms several state-of-the-art FCN-based methods, demonstrating that our proposed method may provide important clues to reveal the underlying interactions of brain regions, and thereby contribute to the understanding of disease neuropathology and the development of diagnostic imaging.

Furthermore, we found that the functional connectivity constructed by the proposed wck-CNN method is significantly different between patient and HC groups, suggesting that this functional connectivity could convey important interaction information for brain function analysis. Also, this connectivity mainly focuses

on specific disease-related brain regions that have been widely reported in previous studies, including lateral surface (Buckner et al., 2009), parietal lobe (Buckner et al., 2009; Han et al., 2012), limbic lobe (Zhou et al., 2008; Ni et al., 2017) and sub cortical gray nuclei (Yao et al., 2013; Liu et al., 2012). For example, it has been reported that the activity in the default mode network (including the brain regions of posterior cingulate gyrus, hippocampus and middle frontal gyrus) might be directly related to the pathology of AD (Buckner et al., 2008; Klaassens et al., 2017). Also, we found more significant changes in functional connectivity for the AD patients compared with eMCI patients, suggesting that the damage of AD on the brain function is gradually enhanced along the disease progress.

Finally, we found that, compared with the traditional FCNs, the dynamic FCNs can achieve better results in automated brain disease diagnosis. This indicates that the dynamics of functional connectivity might be linked with the changes of brain function and cognitive ability.

It is worth noting that, besides the FCN construction and disease diagnosis, our proposed wck-CNN method provides an approach to measure the changing properties of dynamic FCNs. So far, the latter task is still challenging due to the complexity of the human brain. Our results show that, compared with the features learned by the competing methods, the features learned by our wck-CNN method are more discriminative, and thus can yield better classification performance. This suggests that our proposed wck-CNN method can capture the important network properties and thus could be used for measuring the changing properties of dynamic FCNs. Besides, our proposed wck-CNN method is a general FCN-based CNN framework, which can also be applied to other FCN-based analysis tasks, such as regression/prediction of some clinical scores (e.g., MMSE) and age.

5.2. Effect of size of proposed wc-kernel

It has been suggested that functional connectivity around 30–60 s of fMRI data can produce robust results in brain connectivity network analysis (Jones et al., 2012; Shirer et al., 2012). In our proposed wc-kernel, the parameter L_1 determines kernel size (*i.e.*, the number of time points) in functional connectivity network construction. To investigate the effects of this parameter on classification performance of our proposed wck-CNN method, we test different values for the parameter L_1 from {20, 40, 70}. Fig. 7 plots the classification accuracy with respect to different L_1 values. For comparison, in Fig. 7 we also give the classification accuracy of other two dynamic FCN based methods (*i.e.*, wck-CNN-1 and DFCN-CNN) with respect to different kernel sizes or sliding window lengths (*i.e.*, $L_1 = \{20, 40, 70\}$ in the wck-CNN-1 method and sliding window length equaling to {20, 40, 70} in the DFCN-CNN method).

As we can see from Fig. 7, for all parameter values, our proposed wck-CNN method consistently outperforms methods of wck-CNN-1 and DFCN-CNN on three classification tasks, further suggesting the efficacy of our proposed wck-CNN method. Also, the classification performance of two wc-kernel based methods (*i.e.*, wck-CNN and wck-CNN-1) outperforms DFCN-CNN method, which shows the effectiveness of our defined wc-kernel in conveying the interactions of brain regions. Moreover, from Fig. 7 we can see that, the classification accuracies of the proposed wck-CNN on three classification tasks are little affected with different parameter values of L_1, indicating our proposed method is very robust for the wc-kernel size.

5.3. Effect of multiple scans of subjects

Because we have only a limited number of subjects, we use all scans (at all stages) of training subjects as independent samples to train different models in the experiments. To evaluate the effect of this step, we test the classification performance of our proposed wck-CNN method using only one scan of each training subject. Specifically, we use the baseline scan of training subjects as training data to train the proposed wck-CNN model. The results show that the proposed wck-CNN method only using the baseline scans yields the accuracies of 72.7%, 78.5% and 45.6% for eMCI vs. HC, AD vs. HC, and AD vs. lMCI vs. eMCI vs. HC classification tasks, respectively. These results are inferior to those of the proposed wck-CNN method using all scans at all stages of training subjects, indicating that it using more scans can enhance the generalization ability of the model.

5.4. Limitations

Although our proposed method achieves good performance in both FCN construction and diagnosis, this study is limited by the following three aspects. *First*, the neurobiological basis for fluctuations in functional connectivity overtime is still unclear (Kudela et al., 2017; Zhang et al., 2016). In spite of the large studies in dynamic FCNs, researchers find it difficult to determine which fluctuations are actually due to neuronal activity or just noise. *Second*, brain parcellation (*i.e.*, the definition of brain regions) is the very basic step for FCN construction and analysis, and we apply the AAL template to brain parcellation in the current study, while using different brain parcellations will yield different brain networks with different connectivity (Zalesky et al., 2010). In our future work, we will evaluate the influence of using different brain parcellations on the performance of our proposed method. *Third*, the size of the dataset is small, although we use all scans of all subjects with rs-fMRI data from ADNI. As our future work, we will evaluate our proposed method on larger datasets with brain diseases other than AD, such as attention deficit hyperactivity disorder (ADHD). *Third*, the size of the dataset is small, and the dataset used in this studies, although we use all scans of all subjects with rs-fMRI data from ADNI. As our future work, we will evaluate our proposed method on larger datasets with brain diseases other than AD, such as attention deficit hyperactivity disorder (ADHD). *Fourth*, in our experiments, we validate the proposed model on subjects with multiple different scan parameters, which could affect the generalization of the proposed method. As the further work, we will evaluate the performance of the proposed method on datasets with the same scan parameter. *Finally*, due to the limitation of ADNI data, in this study, we could not provide the exact amyloid/tau on PET/CSF to obtain the percent of MCI with evidence of AD pathophysiology.

6. Conclusion

In this paper, we define a novel wc-kernel for characterizing rich interaction information between brain regions. Different previous methods (*e.g.*, PCC method) that equally treat all time points, our proposed wc-kernel measures the correlation of brain regions, with learned weights to characterize specific contributions of different time points. We further build a wc-kernel based CNN framework for dynamic FCN construction and analysis using fMRI data. Experimental results on the ADNI dataset demonstrate the effectiveness of our proposed method.

Declaration of Competing Interest

The authors declare that they have no known competing financial interests or personal relationships that could have appeared to influence the work reported in this paper.

Acknowledgment

This study was supported by National Natural Science Foundation of China (nos. 61976006, 61573023, 61703301, 61902003), Foundation for Outstanding Young in Higher Education of Anhui, China (gxyqZD2017010), NGII Fund, China (no. NGII20190612), and AHNU Fundamental Research Funds (nos. 1708085MF145, 1808085MF171).

Supplementary material

Supplementary material associated with this article can be found, in the online version, at doi:10.1016/j.media.2020.101709.

References

Aerts, H., Fias, W., Caeyenberghs, K., Marinazzo, D., 2016. Brain networks under attack: robustness properties and the impact of lesions. Brain 139 (12), 3063–3083.
Arbabshirani, M.R., Kiehl, K.A., Pearlson, G.D., Calhoun, V.D., 2013. Classification of schizophrenia patients based on resting-state functional network connectivity. Front. Neurosci. 7 (133), 1–16.
Bai, F., Liao, W., Watson, D.R., Shi, Y., Wang, Y., Yue, C., Teng, Y., Wu, D., Yuan, Y., Jia, J., et al., 2011. Abnormal whole-brain functional connection in amnestic mild cognitive impairment patients. Behav. Brain Res. 216 (2), 666–672.
Bai, F., Zhang, Z., Watson, D.R., Yu, H., Shi, Y., Yuan, Y., Zang, Y., Zhu, C., Qian, Y., 2009. Abnormal functional connectivity of hippocampus during episodic memory retrieval processing network in amnestic mild cognitive impairment. Biol. Psychiatry 65 (11), 951–958.
Baldaçara, L., Borgio, J.G.F., Moraes, W.A.d.S., Lacerda, A.L.T., Montaño, M.B.M.M., Tufik, S., Bressan, R.A., Ramos, L.R., Jackowski, A.P., 2011. Cerebellar volume in patients with dementia. Revista Brasileira de Psiquiatria 33 (2), 122–129.
Buckner, R.L., Andrews-Hanna, J.R., Schacter, D.L., 2008. The brain's default network. Ann. N. Y. Acad. Sci. 1124 (1), 1–38.
Buckner, R.L., Sepulcre, J., Talukdar, T., Krienen, F.M., Liu, H., Hedden, T., Andrews-Hanna, J.R., Sperling, R.A., Johnson, K.A., 2009. Cortical hubs revealed by intrinsic functional connectivity: mapping, assessment of stability, and relation to Alzheimer's disease. J. Neurosci. 29 (6), 1860–1873.
Bullmore, E., Horwitz, B., Honey, G., Brammer, M., Williams, S., Sharma, T., 2000. How good is good enough in path analysis of fMRI data? Neuroimage 11 (4), 289–301.
Catie Chang, G.H.G., 2010. Time-frequency dynamics of resting-state brain connectivity measured with fMRI. Neuroimage 50 (1), 81–98.
Chang, C., Liu, Z., Chen, M.C., Liu, X., Duyn, J.H., 2013. EEG correlates of time-varying BOLD functional connectivity. Neuroimage 72, 227–236.
Chen, G., Ward, B.D., Xie, C., Li, W., Wu, Z., Jones, J.L., Franczak, M., Antuono, P., Li, S.-J., 2011. Classification of Alzheimer disease, mild cognitive impairment, and normal cognitive status with large-scale network analysis based on resting-state functional MR imaging. Radiology 259 (1), 213–221.
Chen, X., Han, Z., Lee, S.W., Shen, D., 2017. Hierarchical high-order functional connectivity networks and selective feature fusion for mci classification. Neuroinformatics 15 (3), 1–14.
Córdova-Palomera, A., Kaufmann, T., Persson, K., Alnæs, D., Doan, N.T., Moberget, T., Lund, M.J., Barca, M.L., Engvig, A., Brækhus, A., et al., 2017. Disrupted global metastability and static and dynamic brain connectivity across individuals in the Alzheimer's disease continuum. Sci. Rep. 7, 40268:1–14.
Damaraju, E., Allen, E., Belger, A., Ford, J., McEwen, S., Mathalon, D., Mueller, B., Pearlson, G., Potkin, S., Preda, A., et al., 2014. Dynamic functional connectivity analysis reveals transient states of dysconnectivity in schizophrenia. NeuroImage 5, 298–308.
Dvorak, P., Menze, B., 2015. Structured prediction with convolutional neural networks for multimodal brain tumor segmentation. In: Proceeding of the Multimodal Brain Tumor Image Segmentation Challenge, the 18st International Conference on Medical Image Computing and Computer Assisted Intervention, pp. 13–24.
Fox, M.D., Snyder, A.Z., Vincent, J.L., Corbetta, M., Van Essen, D.C., Raichle, M.E., 2005. The human brain is intrinsically organized into dynamic, anticorrelated functional networks. Proc. Natl. Acad. Sci. U.S.A. 102 (27), 9673–9678.
Friston, K.J., Harrison, L., Penny, W., 2003. Dynamic causal modelling.. Neuroimage 19 (4), 1273–1302.
Greicius, M.D., Krasnow, B., Reiss, A.L., Menon, V., 2003. Functional connectivity in the resting brain: a network analysis of the default mode hypothesis. Proc. Natl. Acad. Sci. 100 (1), 253–258.
Greicius, M.D., Srivastava, G., Reiss, A.L., Menon, V., 2004. Default-mode network activity distinguishes Alzheimer's disease from healthy aging: evidence from functional MRI. Proc. Natl. Acad. Sci. U.S.A. 101 (13), 4637–4642.
Guye, M., Bettus, G., Bartolomei, F., Cozzone, P.J., 2010. Graph theoretical analysis of structural and functional connectivity MRI in normal and pathological brain networks. Magn. Reson. Mater. Phys., Biol. Med. 23 (5–6), 409–421.
Han, S.D., Arfanakis, K., Fleischman, D.A., Leurgans, S.E., Tuminello, E.R., Edmonds, E.C., Bennett, D.A., 2012. Functional connectivity variations in mild cognitive impairment: associations with cognitive function. J. Int. Neuropsychol.Soc. 18 (1), 39–48.
Henaff, M., Bruna, J., Lecun, Y., 2015. Deep Convolutional Networks on Graph-Structured Data. arXiv preprint, 1–10.
Hinton, G. E., Srivastava, N., Krizhevsky, A., Sutskever, I., Salakhutdinov, R. R., 2012. Improving neural networks by preventing co-adaptation of feature detectors. arXiv preprint arXiv:1207.0580.
Hutchison, R.M., Womelsdorf, T., Allen, E.A., Bandettini, P.A., Calhoun, V.D., Corbetta, M., Della Penna, S., Duyn, J.H., Glover, G.H., Gonzalez-Castillo, J., et al., 2013. Dynamic functional connectivity: promise, issues, and interpretations. Neuroimage 80, 360–378.
Jie, B., Liu, M., Shen, D., 2018. Integration of temporal and spatial properties of dynamic connectivity networks for automatic diagnosis of brain disease. Med. Image Anal. 47, 81–94.
Jie, B., Zhang, D., Gao, W., Wang, Q., Wee, C.-Y., Shen, D., 2014. Integration of network topological and connectivity properties for neuroimaging classification. IEEE Trans. Biomed. Eng. 61 (2), 576–589.
Jie, B., Zhang, D., Wee, C.-Y., Shen, D., 2014. Topological graph kernel on multiple thresholded functional connectivity networks for mild cognitive impairment classification. Hum. Brain Mapp. 35 (7), 2876–2897.
Jones, D.T., Vemuri, P., Murphy, M.C., Gunter, J.L., Senjem, M.L., Machulda, M.M., Przybelski, S.A., Gregg, B.E., Kantarci, K., Knopman, D.S., et al., 2012. Non-stationarity in the "resting brain's" modular architecture. PLoS ONE 7 (6), e39731:1–15.
Kawahara, J., Brown, C.J., Miller, S.P., Booth, B.G., Chau, V., Grunau, R.E., Zwicker, J.G., Hamarneh, G., 2016. Brainnetcnn: convolutional neural networks for brain networks; towards predicting neurodevelopment. Neuroimage 146, 1038–1049.
Kiviniemi, V., Vire, T., Remes, J., Elseoud, A.A., Starck, T., Tervonen, O., Nikkinen, J., 2011. A sliding time-window ICA reveals spatial variability of the default mode network in time. Brain Connect. 1 (4), 339–347.
Klaassens, B.L., Jma, V.G., Van, d.G.J., De, V.F., Müller, C., Sarb, R., 2017. Diminished posterior precuneus connectivity with the default mode network differentiates normal aging from alzheimer's disease.. Front. Aging Neurosci. 9, 1–13.
Kucyi, A., Davis, K.D., 2014. Dynamic functional connectivity of the default mode network tracks daydreaming. Neuroimage 100, 471–480.
Kudela, M., Harezlak, J., Lindquist, M.A., 2017. Assessing uncertainty in dynamic functional connectivity. Neuroimage 149, 165–177.
Lian, C., Liu, M., Zhang, J., Shen, D., 2019. Hierarchical fully convolutional network for joint atrophy localization and Alzheimer's disease diagnosis using structural MRI. IEEE Trans. Pattern Anal. Mach. Intell..
Lian, C., Zhang, J., Liu, M., Zong, X., Hung, S.-C., Lin, W., Shen, D., 2018. Multi-channel multi-scale fully convolutional network for 3D perivascular spaces segmentation in 7t MR images. Med. Image Anal. 46, 106–117.
Liu, M., Zhang, J., Adeli, E., Shen, D., 2017. Landmark-based deep multi-instance learning for brain disease diagnosis. Med. Image Anal. 43, 157–168.
Liu, M., Zhang, J., Nie, D., Yap, P.-T., Shen, D., 2018. Anatomical landmark based deep feature representation for MR images in brain disease diagnosis. IEEE J. Biomed. Health Inform. 22 (5), 1476–1485.
Liu, Z., Zhang, Y., Yan, H., Bai, L., Dai, R., Wei, W., Zhong, C., Xue, T., Wang, H., Feng, Y., et al., 2012. Altered topological patterns of brain networks in mild cognitive impairment and Alzheimer's disease: a resting-state fMRI study. Psychiatry Res. 202 (2), 118–125.
Ni, H., Qin, J., Zhou, L., Zhao, Z., Wang, J., Hou, F., (ADNI, A.D.N.I., et al., 2017. Network analysis in detection of early-stage mild cognitive impairment. Physica A 478, 113–119.
Ohiorhenuan, I.E., Mechler, F., Purpura, K.P., Schmid, A.M., Hu, Q., Victor, J.D., 2010. Sparse coding and high-order correlations in fine-scale cortical networks. Nature 466 (7306), 617–621.
Pan, Y., Liu, M., Lian, C., Xia, Y., Shen, D., 2019. Disease-image specific generative adversarial network for brain disease diagnosis with incomplete multi-modal neuroimages. In: International Conference on Medical Image Computing And Computer Assisted Intervention, pp. 1–9.
Pan, Y., Liu, M., Lian, C., Zhou, T., Xia, Y., Shen, D., 2018. Synthesizing missing PET from MRI with cycle-consistent generative adversarial networks for Alzheimer's disease diagnosis. In: International Conference on Medical Image Computing and Computer-Assisted Intervention. Springer, pp. 455–463.
Preti, M.G., Bolton, T.A., Van De Ville, D., 2017. The dynamic functional connectome: state-of-the-art and perspectives. Neuroimage 160, 41–54.
Qiao, L., Zhang, L., Chen, S., Shen, D., 2018. Data-driven graph construction and graph learning: areview. Neurocomputing 312, 336–351.
Sadaghiani, S., Hesselmann, G., Friston, K.J., Kleinschmidt, A., 2010. The relation of ongoing brain activity, evoked neural responses, and cognition. Front. Syst. Neurosci. 4 (20), 1–14.
Sadaghiani, S., Kleinschmidt, A., 2013. Functional interactions between intrinsic brain activity and behavior. Neuroimage 80 (2), 379–386.
Sakoglu, U., Michael, A., Calhoun, V., 2009. Classification of schizophrenia patients vs healthy controls with dynamic functional network connectivity. Neuroimage 47 (1), S39–S41.
Sakoğlu, Ü., Pearlson, G.D., Kiehl, K.A., Wang, Y.M., Michael, A.M., Calhoun, V.D., 2010. A method for evaluating dynamic functional network connectivity and task-modulation: application to schizophrenia. Magn. Reson. Mater. Phys., Biol. Med. 23 (5–6), 351–366.
Sanz-Arigita, E.J., Schoonheim, M.M., Damoiseaux, J.S., Rombouts, S.A., Maris, E., Barkhof, F., Scheltens, P., Stam, C.J., 2010. Loss of 'small-world' networks in Alzheimer's disease: graph analysis of fMRI resting-state functional connectivity. PLoS ONE 5 (11), e13788:1–14.

Seeley, W.W., Crawford, R.K., Zhou, J., Miller, B.L., Greicius, M.D., 2009. Neurodegenerative diseases target large-scale human brain networks. Neuron 62 (1), 42–52.
Shirer, W., Ryali, S., Rykhlevskaia, E., Menon, V., Greicius, M., 2012. Decoding subject-driven cognitive states with whole-brain connectivity patterns. Cerebral Cortex 22 (1), 158–165.
Smith, S.M., Miller, K.L., Salimi-Khorshidi, G., Webster, M., Beckmann, C.F., Nichols, T.E., Ramsey, J.D., Woolrich, M.W., 2011. Network modelling methods for fMRI. Neuroimage 54 (2), 875–891.
Sporns, O., 2011. The human connectome: a complex network. Ann. N. Y. Acad. Sci. 1224 (1), 109–125.
Stam, C., Jones, B., Nolte, G., Breakspear, M., Scheltens, P., 2007. Small-world networks and functional connectivity in alzheimer's disease. Cerebral Cortex 17 (1), 92–99.
Starck, T., Nikkinen, J., Rahko, J., Remes, J., Hurtig, T., Haapsamo, H., Jussila, K., Kuusikko-Gauffin, S., Mattila, M.-L., Jansson-Verkasalo, E., et al., 2013. Resting state fMRI reveals a default mode dissociation between retrosplenial and medial prefrontal subnetworks in ASD despite motion scrubbing. Front. Hum. Neurosci. 7 (802), 1–10.
Supekar, K., Menon, V., Rubin, D., Musen, M., Greicius, M.D., 2008. Network analysis of intrinsic functional brain connectivity in alzheimer's disease. PLoS Comput. Biol. 4 (6), e1000100:1–11.
Tagliazucchi, E., Balenzuela, P., Fraiman, D., Chialvo, D.R., 2012. Criticality in large-scale brain fMRI Dynamics unveiled by a novel point process analysis. Front. Physiol. 3 (15), 1–12.
Tagliazucchi, E., Balenzuela, P., Fraiman, D., Montoya, P., Chialvo, D.R., 2011. Spontaneous bold event triggered averages for estimating functional connectivity at resting state. Neurosci. Lett. 488 (2), 158–163.
Thompson, G.J., Magnuson, M.E., Merritt, M.D., Schwarb, H., Pan, W.-J., McKinley, A., Tripp, L.D., Schumacher, E.H., Keilholz, S.D., 2013. Short-time windows of correlation between large-scale functional brain networks predict vigilance intraindividually and interindividually. Hum. Brain Mapp. 34 (12), 3280–3298.
Tzourio-Mazoyer, N., Landeau, B., Papathanassiou, D., Crivello, F., Etard, O., Delcroix, N., Mazoyer, B., Joliot, M., 2002. Automated anatomical labeling of activations in SPM using a macroscopic anatomical parcellation of the MNI MRI single-subject brain. Neuroimage 15 (1), 273–289.
Uddin, L.Q., Supekar, K., Lynch, C.J., Khouzam, A., Phillips, J., Feinstein, C., Ryali, S., Menon, V., 2013. Salience network-based classification and prediction of symptom severity in children with autism. JAMA Psychiatry 70 (8), 869–879.
Van Dijk, K.R., Sabuncu, M.R., Buckner, R.L., 2012. The influence of head motion on intrinsic functional connectivity MRI. Neuroimage 59 (1), 431–438.
Wang, J., Zuo, X., Dai, Z., Xia, M., Zhao, Z., Zhao, X., Jia, J., Han, Y., He, Y., 2013. Disrupted functional brain connectome in individuals at risk for Alzheimer's disease. Biol. Psychiatry 73 (5), 472–481.
Wang, M., Huang, J., Liu, M., Zhang, D., 2019. Functional connectivity network analysis with discriminative hub detection for brain disease identification. In: Proceedings of the AAAI Conference on Artificial Intelligence, 33, pp. 1198–1205.
Wang, M., Zhang, D., Huang, J., Yap, P.-T., Shen, D., Liu, M., 2019. Identifying autism spectrum disorder with multi-site fMRI via low-rank domain adaptation. IEEE Trans. Med. Imaging.
Wee, C.-Y., Yang, S., Yap, P.-T., Shen, D., Initiative, A.D.N., et al., 2016. Sparse temporally dynamic resting-state functional connectivity networks for early MCI identification. Brain Imaging Behav. 10 (2), 342–356.
Wee, C.-Y., Yap, P.-T., Li, W., Denny, K., Browndyke, J.N., Potter, G.G., Welsh-Bohmer, K.A., Wang, L., Shen, D., 2011. Enriched white matter connectivity networks for accurate identification of MCI patients. Neuroimage 54 (3), 1812–1822.
Wee, C.-Y., Yap, P.-T., Wang, L., Shen, D., 2014. Group-constrained sparse fMRI connectivity modeling for mild cognitive impairment identification. Brain Struct. Funct. 219 (2), 641–656.
Wee, C.-Y., Yap, P.-T., Zhang, D., Denny, K., Browndyke, J.N., Potter, G.G., Welsh-Bohmer, K.A., Wang, L., Shen, D., 2012. Identification of MCI individuals using structural and functional connectivity networks. Neuroimage 59 (3), 2045–2056.
Wee, C.-Y., Yap, P.-T., Zhang, D., Denny, K., Browndyke, J.N., Potter, G.G., Welsh-Bohmer, K.A., Wang, L., Shen, D., 2012. Identification of MCI individuals using structural and functional connectivity networks. Neuroimage 59 (3), 2045–2056.
Wee, C.-Y., Zhao, Z., Yap, P.-T., Wu, G., Shi, F., Price, T., Du, Y., Xu, J., Zhou, Y., Shen, D., 2014. Disrupted brain functional network in internet addiction disorder: a resting-state functional magnetic resonance imaging study. PLoS ONE 9 (9), e107306:1–11.
Weis, S., Klaver, P., Reul, J., Elger, C.E., Fernández, G., 2004. Temporal and cerebellar brain regions that support both declarative memory formation and retrieval. Cerebral Cortex 14 (3), 256–267.
Wen, H., Liu, Y., Rekik, I., Wang, S., Chen, Z., Zhang, J., Zhang, Y., Peng, Y., He, H., 2018. Combining disrupted and discriminative topological properties of functional connectivity networks as neuroimaging biomarkers for accurate diagnosis of early tourette syndrome children. Mol. Neurobiol. 55 (4), 3251–3269.
Xiang, L., Wang, Q., Nie, D., Zhang, L., Jin, X., Qiao, Y., Shen, D., 2018. Deep embedding convolutional neural network for synthesizing CT image from T1-weighted MR image. Med. Image Anal. 47, 31–44.
Yao, H., Liu, Y., Zhou, B., Zhang, Z., An, N., Wang, P., Wang, L., Zhang, X., Jiang, T., 2013. Decreased functional connectivity of the amygdala in Alzheimer's disease revealed by resting-state fmri. Eur. J. Radiol. 82 (9), 1531–1538.
Yu, S., Yang, H., Nakahara, H., Santos, G.S., Nikoli, D., Plenz, D., 2011. Higher-order interactions characterized in cortical activity. J. Neurosci. Of. J.Soc. Neurosci. 31 (48), 17514–17526.
Zalesky, A., Fornito, A., Cocchi, L., Gollo, L.L., Breakspear, M., 2014. Time-resolved resting-state brain networks. Proc. Natil. Acad. Sci. 111 (28), 10341–10346.
Zalesky, A., Fornito, A., Harding, I.H., Cocchi, L., Yücel, M., Pantelis, C., Bullmore, E.T., 2010. Whole-brain anatomical networks: does the choice of nodes matter? Neuroimage 50 (3), 970–983.
Zanin, M., Sousa, P., Papo, D., Bajo, R., Garcia-Prieto, J., del Pozo, F., Menasalvas, E., Boccaletti, S., 2012. Optimizing functional network representation of multivariate time series. Sci. Rep. 2 (630), 1–7.
Zhang, D., Huang, J., Jie, B., Du, J., Tu, L., Liu, M., 2018. Ordinal pattern: a new descriptor for brain connectivity networks. IEEE Trans. Med. Imaging 37 (7), 1711–1722.
Zhang, J., Cheng, W., Liu, Z., Zhang, K., Lei, X., Yao, Y., Becker, B., Liu, Y., Kendrick, K.M., Lu, G., et al., 2016. Neural, electrophysiological and anatomical basis of brain-network variability and its characteristic changes in mental disorders. Brain 139 (8), 2307–2321.
Zhang, J., Small, M., 2006. Complex network from pseudoperiodic time series: topology versus dynamics. Phys. Rev. Lett. 96 (23), 238701:1–4.
Zhou, Y., Dougherty, J.H., Hubner, K.F., Bai, B., Cannon, R.L., Hutson, R.K., 2008. Abnormal connectivity in the posterior cingulate and hippocampus in early Alzheimer's disease and mild cognitive impairment. Alzheimer's Dementia 4 (4), 265–270.
Zhu, Y., Wang, L., Liu, M., Qian, C., Yousuf, A., Oto, A., Shen, D., 2017. MRI-based prostate cancer detection with high-level representation and hierarchical classification. Med. Phys. 44 (3), 1028–1039.